Article

Design of a Nickel-Based Bond-Coat Alloy for Thermal Barrier Coatings on Copper Substrates

Torben Fiedler *, Tatiana Fedorova, Joachim Rösler and Martin Bäker

Institute for Materials, Technische Universität Braunschweig, Langer Kamp 8,
38106 Braunschweig, Germany; E-Mails: t.fedorova@tu-bs.de (T.F.); j.roesler@tu-bs.de (J.R.);
martin.baeker@tu-bs.de (M.B.)

* Author to whom correspondence should be addressed; E-Mail: t.fiedler@tu-bs.de;
  Tel.: +49-531-391-3063.

Abstract: To increase the lifetime of rocket combustion chambers, thermal barrier coatings (TBC) may be applied on the copper chamber wall. Since standard TBC systems used in gas turbines are not suitable for rocket-engine application and fail at the interface between the substrate and bond coat, a new bond-coat material has to be designed. This bond-coat material has to be chemically compatible to the copper substrate to improve the adhesion and needs a coefficient of thermal expansion close to that of copper to reduce thermal stresses. One approach to achieve this is to modify the standard NiCrAlY alloy used in gas turbines by adding copper. In this work, the influence of copper on the microstructure of NiCrAlY-alloys is investigated with thermodynamical calculations, optical microscopy, SEM, EDX and calorimetry. Adding copper leads to the formation of a significant amount of β-NiAl and α-Cr. Reducing the aluminum and chromium content leads furthermore to a two-phase fcc microstructure.

Keywords: thermal barrier coatings; CuNiCrAl; rocket engine; copper nickel chromium aluminum; CTE; Thermo-Calc

1. Introduction

The combustion chamber in rocket engines has to withstand high thermomechanical loads. To cool down the chamber wall, it is usually made out of a Cu-alloy with high thermal conductivity. Although the material is chilled inside by liquid hydrogen in cooling channels, surface-temperatures of more than 800 °C are reached [1]. This load may cause damage due to the so-called dog-house-effect [2,3], which is caused by high internal pressure in the cooling channels, thermomechanical fatigue and creep mechanisms. One idea to avoid this damage is to lower the surface temperature of the copper alloy by applying thermal barrier coatings (TBC).

In previous studies, several types of coatings for rocket engines have been tested on copper substrates. Ogbuji *et al.* [4] used a Cu/Cr coating to protect the combustion-chamber material Cu-8%Cr-5%Nb. The coatings showed a lifetime of 10 h at a Cr content of 21%. A NiCrAlY top-coat was investigated by Raj *et al.* [5] using a Cu/Cr bond-coat on a Cu-8%Cr-4%Nb substrate. The coatings were thermally cycled in a H_2/O_2-flame. They showed no failure after 40 cycles, although large internal stresses were calculated with finite element analysis. In Schloesser *et al.* [6], a standard TBC-system used in gas-turbines on Ni-substrates has been tested. It consists of a ceramic yttrium stabilized zirconia top-coat (TC) and a Ni-22%Cr-10%Al-1%Y bond-coat (BC). It was found that a chemical gradient and the mismatch of thermal expansion cause damage at the substrate/BC-interface, although the typical failure in gas-turbines takes place at the BC/TC-interface.

Since the main failure in the previous research took place at the substrate/bond-coat interface, while the top-coat showed no significant failure, further research has to focus on the development of new bond-coat materials. The main goal is to reduce the dissimilarity in chemical composition and the mismatch in the coefficient of thermal expansion (CTE) between bond coat and substrate. The mean CTE (related to room temperature) of the typically used NiCrAlY alloys is about $14 \times 10^{-6} \, \text{K}^{-1}$ at 600 °C and 800 °C [7,8] and $18 \times 10^{-6} \, \text{K}^{-1}$ (600 °C), respectively, $20 \times 10^{-6} \, \text{K}^{-1}$ (800 °C) for copper [8–10]. The mismatch in the CTE here is about $5 \times 10^{-6} \, \text{K}^{-1}$, while the CTE of Ni-based superalloys usually used in gas-turbines does not differ by more than $0.1 \times 10^{-6} \, \text{K}^{-1}$ [11] from the CTE of the bond-coat alloy.

One approach to lower the CTE mismatch and the chemical dissimilarity is to add copper to the NiCrAlY bond-coat alloy, based on the concepts proposed in [12]. Since there is no data available for Cu-NiCrAlY alloys, the binary alloy Ni-Cu was considered for the first evaluation. The Ni-30%Cu alloy was found to have a mean CTE of $16 \times 10^{-6} \, \text{K}^{-1}$ at 600 ×C and $17 \times 10^{-6} \, \text{K}^{-1}$ at 800 °C [8], which is only about $2 \times 10^{-6} \, \text{K}^{-1}$ lower than the CTE of copper. Although a Cu-content higher than 30% leads to a CTE more similar to the CTE of the copper substrate, it will lower the melting temperature and the strength of the alloy.

In this paper, the influence of copper in NiCrAl alloys is investigated at a copper content of 30%. The commonly-used NiCrAlY alloy with a Cr content of 22% and an Al content of 10% is chosen as a reference alloy. This alloy consists of the high-temperature phases γ and β and the low-temperature phases γ' and α. The γ-phase is a Ni-rich fcc-crystal; γ' is a fcc superlattice of the γ-phase with the stoichiometry Ni_3Al in the binary system; while in the ternary Ni-Cr-Al-system, the chromium is able to substitute both, the Al and the Ni atom. The β-phase is an intermetallic cubic structure with the stoichiometry NiAl in the binary Ni-system, and α is a cubic chromium rich phase [13–16].

In this work, possible phase compositions are calculated with CALPHADcalculations. Based on the calculations, different alloys are chosen for further investigation. These alloys are examined metallographically and with calorimetric measurements to compare the observed microstructure with the calculations. A similar approach was used previously to study the influence of Fe [15].

2. Results and Discussion

To compare the results in this work with a well-known alloy system, the alloy Ni-22%Cr-10%Al was chosen as a reference, based on the work of Schloesser in previous studies [6], where the alloy Ni-22%Cr-10%Al-1%Y has been used as a bond-coat material on copper substrates. The alloy there contains yttrium, which improves the adhesion of the aluminum oxide layers and leads to an improved cyclic oxidation behavior. This effect is not of crucial importance in rocket engines due to the short time of hot-gas exposure compared to gas-turbine application [14], and consequently, Yttrium is not considered here. The microstructure of a similar alloy Ni-20%Cr-12%Al has been studied by Achar *et al.* [20].

Figure 1. Calculated phase composition of the reference alloy Ni-22%Cr-10%Al and the reference alloy after adding 30% Cu (Ni-30%Cu-22%Cr-10%Al). (**a**) Ni-22%Cr-10%Al (a similar result was published in [15]); (**b**) Ni-30%Cu-22%Cr-10%Al.

(**a**)   (**b**)
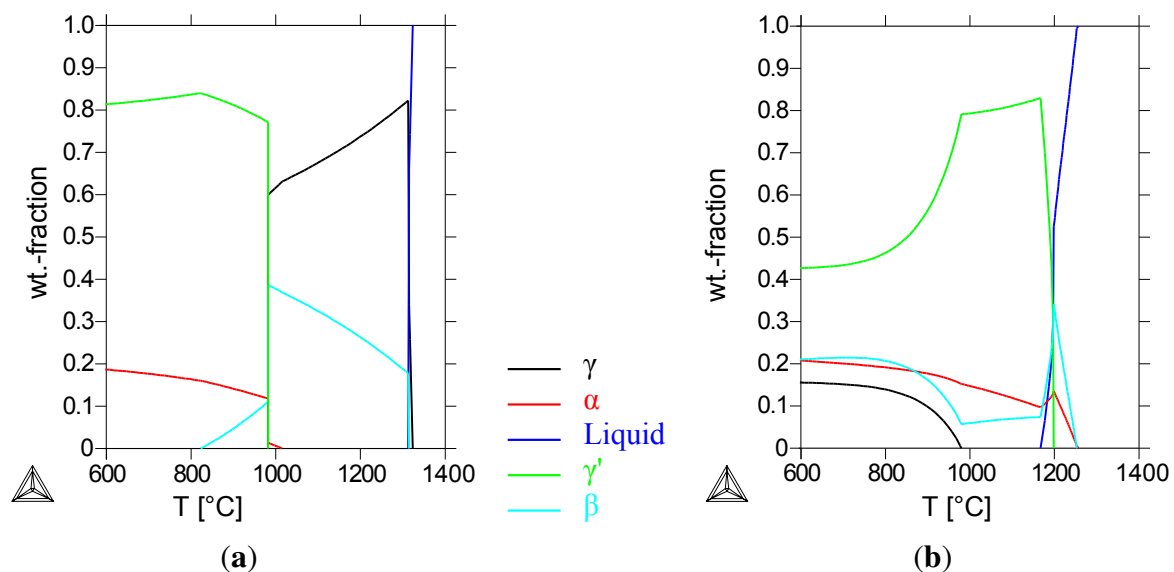
Figure 1(a) shows the calculated phase-composition of the reference alloy. At the homogenization temperature of 1000 °C, a composition of 35% cubic β-NiAl and 65% fcc γ-Ni is calculated. Below 980 °C, the formation of a bcc α-Cr- and an fcc γ'-phase is calculated; the β phase is still present with a fraction of 11 wt%. The calculated β mass-fraction decreases at temperatures lower than 980 °C. At the heat-treatment temperature of 800 °C, the calculated composition of the alloy is only γ' and α-Cr. The calorimetric measurements (Figure 2) showed good agreement with the calculations. Here, the phase-reaction temperature was measured at 985 °C and differs only by 5 K from the calculated temperature. The measured solidus temperature is 1295 °C and differs only by 10 K from the calculated solidus temperature of 1305 °C.

Figure 2. Calorimetric measurement data for the reference alloy Ni-22%Cr-10%Al: heating curve after homogenization.
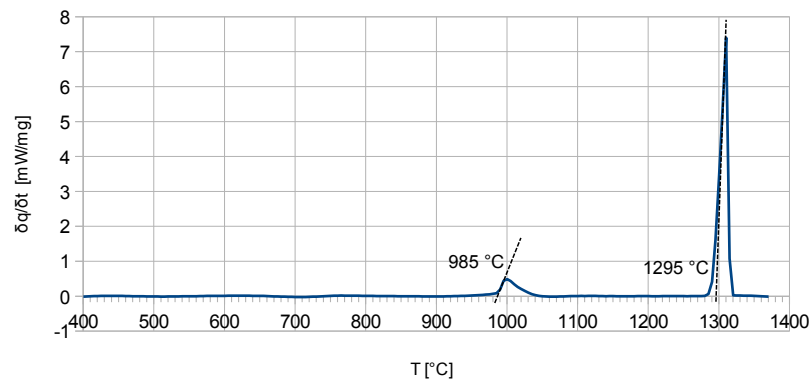

Figure 3. Optical micrographs of the reference-alloy Ni-22%Cr-10%Al after different heat treatments. The samples were quenched in water after each heat treatment and were not etched in this picture. (**a**) Homogenization (1000 °C, 4 h); (**b**) 800 °C, 4 h; (**c**) 800 °C, 100 h.

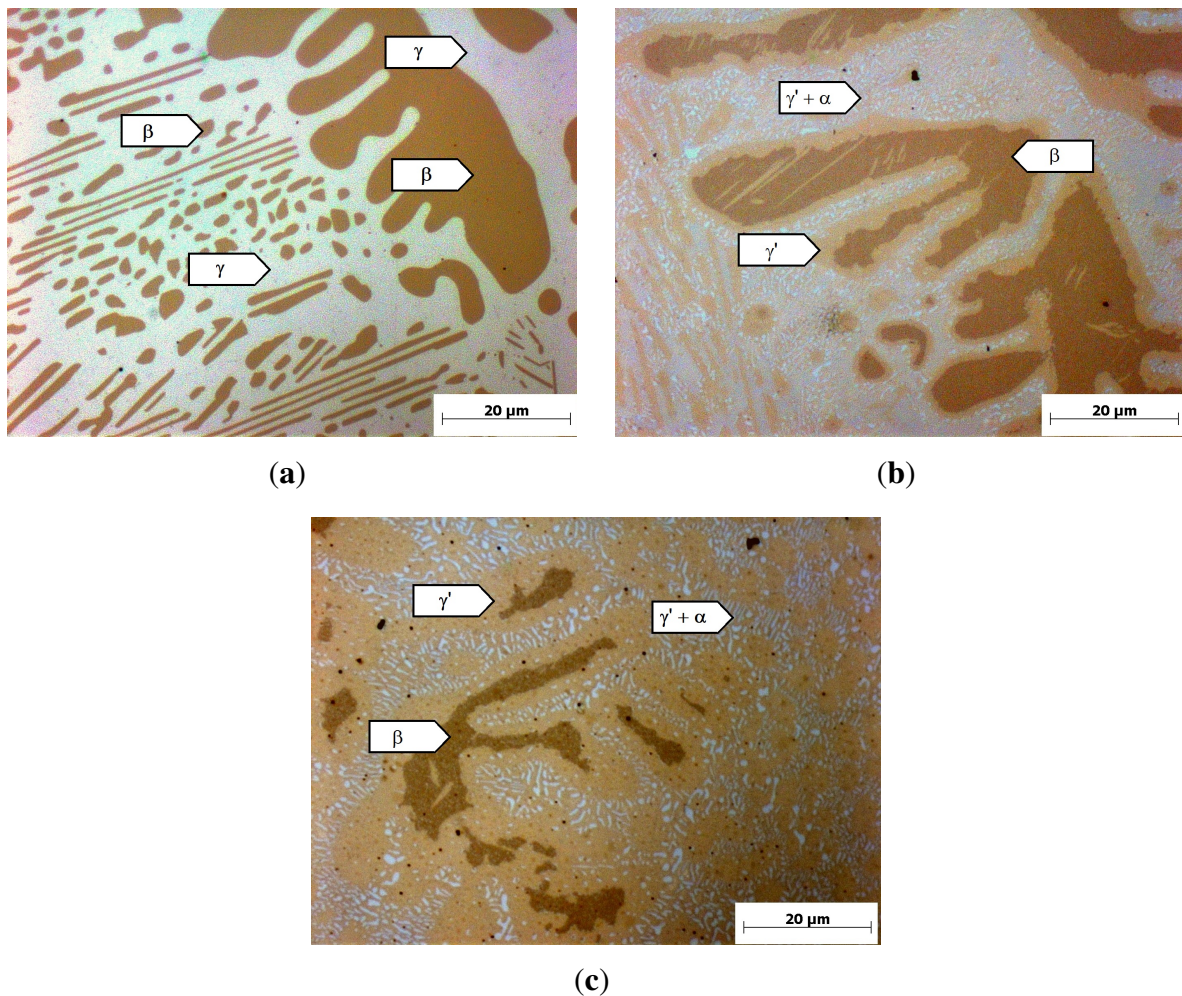
(**a**)

(**b**)

(**c**)

Figure 3(a) shows the micrograph of the reference alloy after casting and homogenization. It consists of a dark brown dendritic phase with a content of 35%, measured with optical image analysis, and a bright interdendritic phase. A similar microstructure has been found by Achar [20] and was there identified as

the cubic β-NiAl (dark brown) and the fcc γ-Ni (bright). Considering the Thermo-Calc calculations and the work of Achar, the dark brown dendritic phase in Figure 3(a) can be identified as β-NiAl and the interdendritic phase as the γ-phase.

After heat treatment at 800 °C, a two-phase γ'/α-Cr microstructure was predicted by the calculations. The metallographic examination (Figure 3(b),(c)) shows that the β-phase is still existent in the microstructure. Furthermore, a light brown phase forms at the interface between the β-phase and the interdendritic area. The interdendritic area consists of a light brown phase with the same contrast as the margin-phase around the β-particles and small, bright precipitates. After 4 h of heat treatment (Figure 3(b)), small β-particles are completely converted to the light brown phase. At bigger β-particles, only a small margin of approximately 2 μm thickness of the light brown phase has formed. Further heat treatment for 100 h showed that the light brown phase grows with longer heat-treatment time, while the β-particle size is reduced (Figure 3(c)). The white particles in the interdendritic areas can be identified as α-Cr, since an EDX-analysis of the white particles shows a Cr-content of >60%. Considering the poor resolution of EDX and the influence of the surrounding material, the Cr-content is even higher than measured. An EDX-analysis of the light brown phase shows an Al-content of 11.1% $\pm$ 0.9%, in agreement with the calculated Al-content of the γ'-phase of 12%. Hence, the light brown phase can be identified as γ', agreeing with the work of Achar [20]. The β-phase is still existent in the microstructure in contrast to the calculation, but the heat treatment for 100 h suggests that further heat treatment will lead to a complete conversion of the β-particles into γ' and α-Cr.

2.1. Increasing Cu-Content

For a rocket-engine application, the bond-coat alloy has to be modified by adding copper, as mentioned above. A copper-content of 30% was set as a starting point for further alloy development, because the coefficient of thermal expansion (CTE) was expected to be in the range of the copper substrate's CTE (see the Introduction). To investigate the influence of copper on the microstructure of NiCrAl alloys, the reference alloy examined above was modified by adding 30% copper.

The Thermo-Calc calculations for this alloy (Figure 1(b)) show a first solidifying α-chromium and β-NiAl phase and a γ'-phase solidifying at 1200 °C. Below 980 °C, a γ-phase forms at the expense of the γ'-phase. Compared to the calculations for the Cu-free alloy, the β-phase is still the NiAl-phase, with a calculated chromium and copper content below 5 wt%. The γ'-phase contains now 30% to 40% copper, depending on the temperature, while the γ-phase consists of more than 90% copper (see Figure 4). The microstructure of this alloy after homogenization is shown in Figure 5(a). It consists of a dark brown dendritic phase with bright particles in a light-brown matrix. Due to the morphology of the phases, it can be expected that the dark brown phase and the white particles solidify at higher temperatures than the light brown phase. The white particles were identified with EDX as chromium precipitates (see Figure 6). The light brown interdendritic phase has a measured composition similar to the calculated composition of the γ'-phase at 1000 °C (Figure 4(a)). The dark brown phase has a measured composition very different from the calculated composition of the β-phase, but solidifies dendritically like the β-phase in the calculation. Furthermore, a β-phase has been observed elsewhere

in the Ni-Cu-Al ternary system at 900 °C, even at aluminum contents below 10% [21]. Hence, it can be assumed that the dark brown phase is actually β.

Figure 4. Phase compositions of the alloy Ni-30%Cu-22%Cr-10%Al: measured with EDX and calculated with Thermo-Calc. (**a**) Calculated phase-compositions and measured compositions at 1000 °C; (**b**) calculated phase-compositions and measured compositions at 800 °C. γ and γ' in the interdendritic area could not be analyzed separately due to the poor resolution of EDX.

(**a**)   (**b**)
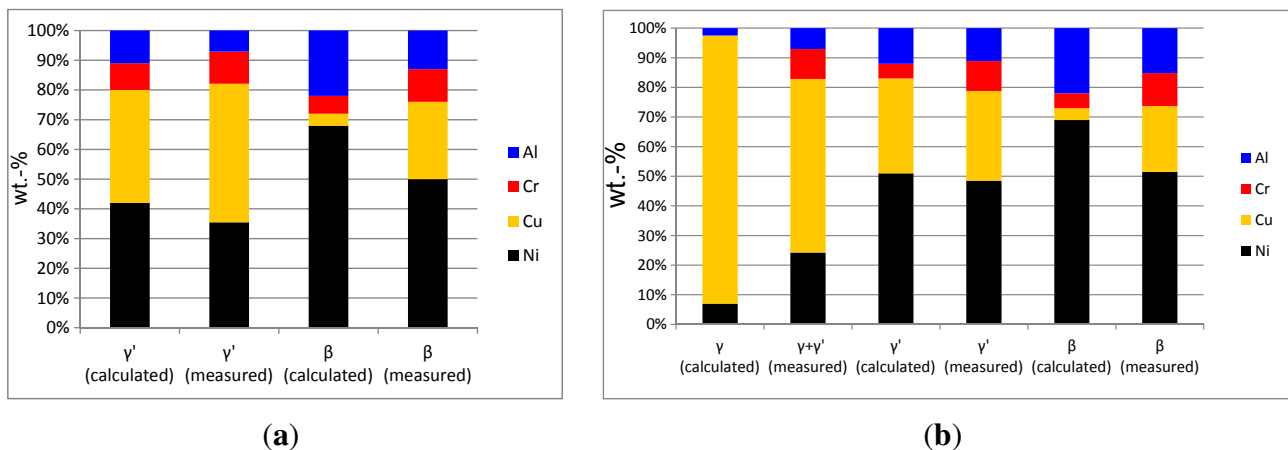
After heat treatment at 800 °C (Figure 5), a light brown phase forms within the interdendritic γ'-phase. Due to the poor resolution of the EDX-measurements, this phase could not be analyzed without the influence of the surrounding γ'-phase. The measured composition of these two phases ($\gamma + \gamma$' in Figure 4(b)) seems to be a mixture between the calculated composition of the γ and γ'-phase. Hence, it can be assumed that at 800 °C, a γ-phase precipitates within the interdendritic γ'-phase, agreeing with the Thermo-Calc calculations in Figure 1(b). Furthermore, a margin around the dark particles was observed at 800 °C, which grows bigger with increasing heat-treatment time. Comparing the location of the small white chromium-particles after homogenization (Figure 5(a)) and after heat treatment at 800 °C (Figure 5), the margin seems to form only out of the β-phase. EDX-measurements at the margin phase show good agreement with the calculated composition of the γ'-phase (Figure 4(b)).

Summing up, the Thermo-Calc calculations show a qualitative agreement with the observed microstructure. Only the quantitative values of phase-composition and fractions differ from the observed values. The reference-alloy with 30% copper consists of a large amount of β-, α- and γ'-phase in the homogenized state. At 800 °C, the γ'-phase forms out of the β-phase. This phase transition will lead to a volumetric change due to the different crystallographic structure [14]. This volumetric change might cause internal stresses. In standard NiCrAlY-alloys, like Ni-22%Cr-10%Al, this has not to be considered, because the phase reaction takes place at 985 ° (see Section 3.1). Furthermore, the CTE of α (9×10^{-6} K^{-1} at 600 °C and 10×10^{-6} K^{-1} at 800 °C) [8] is very low compared to the surrounding γ-, β- and γ'-phase (>15×10^{-6} K^{-1} at 600 °C and 800 °C) [8,22] and will cause additional internal stresses and lower the resulting CTE of the alloy due to mixture rules. For further alloy development, it might be therefore necessary to reduce the amount of β and α-phase.

Figure 5. Optical micrograph of the alloy Ni-30%Cu-22%Cr-10%Al after different heat treatments, not etched. (**a**) Homogenization (1000 °C, 4 h); (**b**) 800 °C, 4 h; (**c**) 800 °C, 100 h.
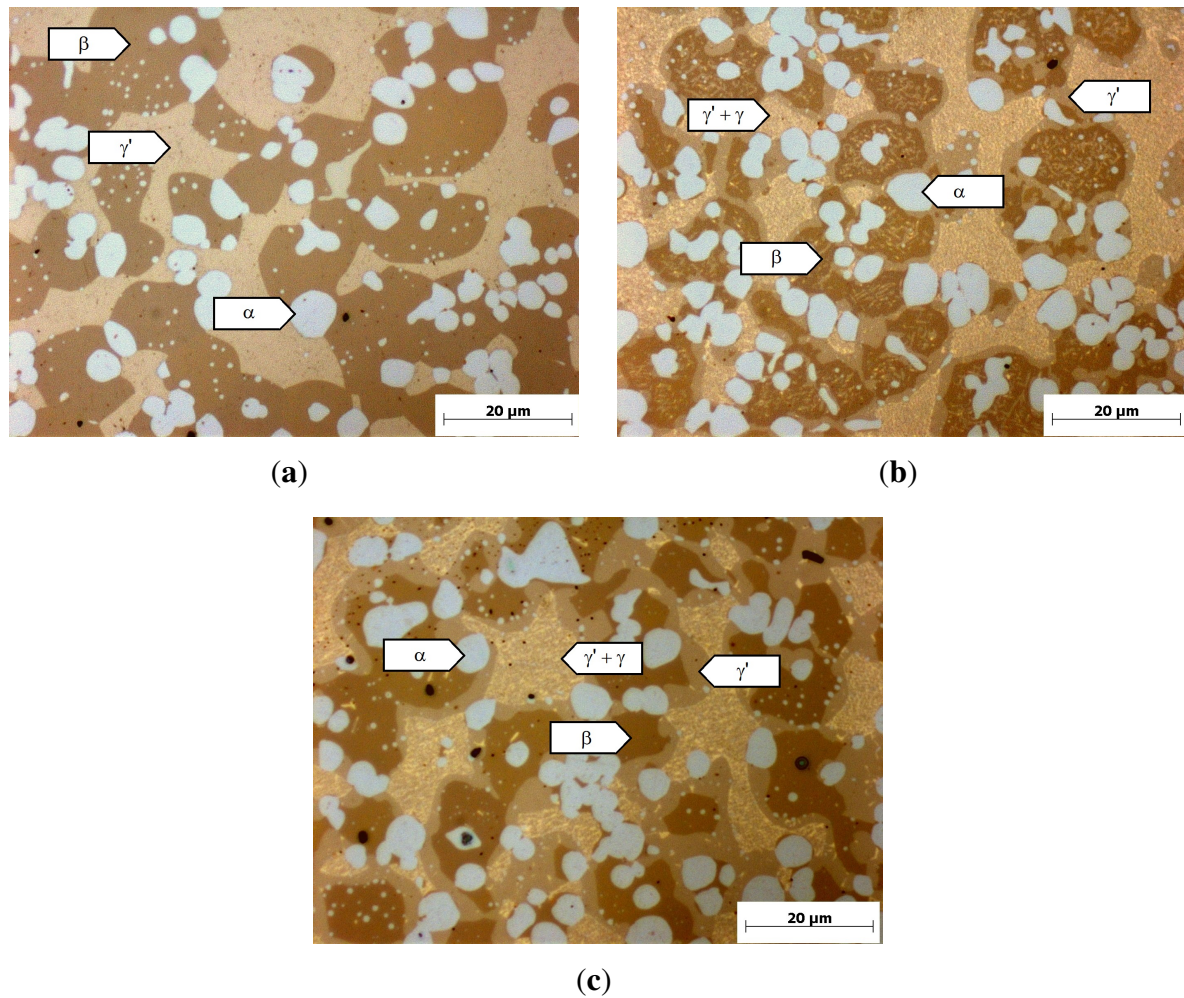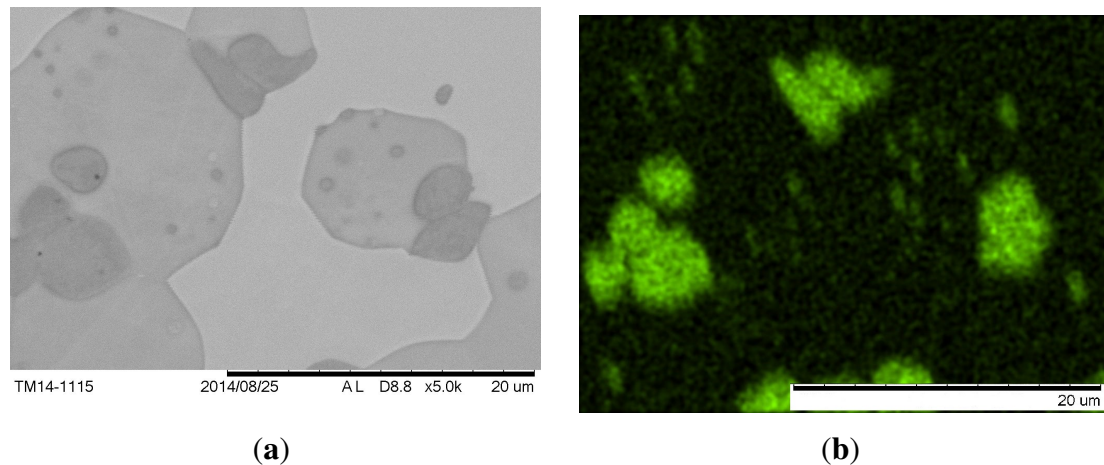

(**a**)

(**b**)

(**c**)

Figure 6. SEM-image of the same sample as in Figure 5(a). (**a**) Back scattered electrons; (**b**) X-ray signals of Cr-Kα.


(**a**)

(**b**)

2.2. Ni-30%Cu-22%Cr

The reference alloy has been modified by adding 30%Cu in the previous section, where an inappropriate amount of α- and β-phase was found, which has to be reduced in further alloy development. The easiest way to eliminate the β-phase in the microstructure is to reduce the aluminum content of the alloy.

The Thermo-Calc calculations in Figure 7 with the Alloy Ni-30%Cu-22%Cr and variable Al-content showed that an Al-content below 8% prevents the formation of the β-phase. According to the calculations, a further reduction of the Al-content below 4% leads to the formation of a second, Cu-rich γ_2-phase. Since most of the copper is dissolved in this γ_2-phase, the Ni-rich γ_1-phase is able to dissolve the chromium. Furthermore, the loss of aluminum increases the total amount of the γ_1-phase, so that the α-Cr-phase destabilizes with the lower Al-content of the alloy. Therefore, one approach for the coating development was to investigate a coating alloy without aluminum, in this case the alloy Ni-30%Cu-22%Cr. Although NiCrAlY bond-coats originally protect the substrate against oxidation by forming a dense Al-oxide layer, it is assumed that the Al-free alloy will form a Cr-oxide layer, which will be sufficient for the short-time hot-gas exposure in rocket engines [12].

Figure 7. Pseudobinary phase diagram calculated by Thermo-Calc of the alloy Ni-30%Cu-22%Cr with variable Al-content. The stable phases are marked with their symbol, phase boundaries with the corresponding color.
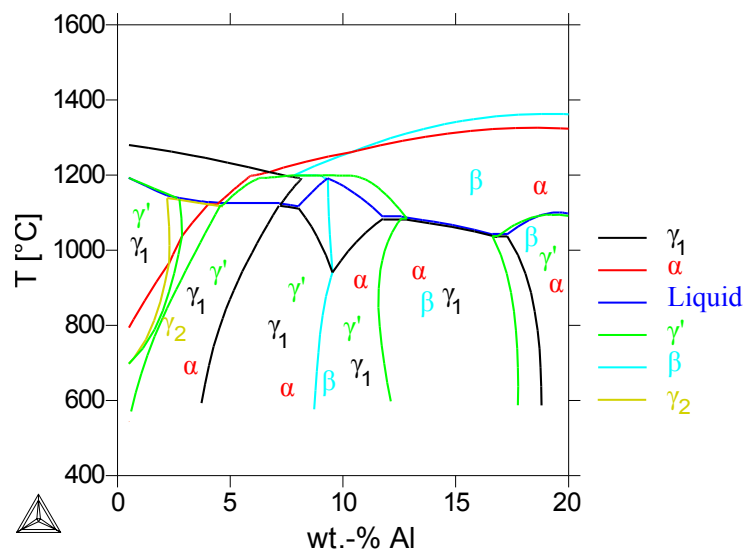
The DSC measurements of the Al-free alloy showed no detectable phase reaction below 1140 °C. The solidus temperature is 1255 °C.

The microstructure after annealing at 1000 °C and etching with molybdic acid is shown in Figure 9(a). It consists of a dendritic phase and an interdendritic phase, which is etched by molybdic acid. The fraction of the phases was measured via optical image analysis; the dendritic phase has a fraction of approximately 70%, agreeing with the calculated value for the first solidifying Ni-rich γ_1-phase. The chemical composition of the dendritic phase measured with EDX is similar to the calculated composition of γ_1, and the measured composition of the interdendritic phase agrees with the calculation of the γ'-phase, respectively (see Figure 10(a)).

The Thermo-Calc calculation of the alloy Ni-30%Cu-22%Cr (Figure 8) showed a two-phase system at temperatures of 800 °C and 1000 °C: a first solidifying Ni-rich γ_1-phase and a second Cu-rich γ'-phase, solidifying at lower temperatures. The γ'-phase converts into a γ_2-phase below 700 °C. The formation of the α-Cr phase is calculated only at temperatures below 750 °C, while in the ternary phase diagram [23], the Cr-phase is even present at temperatures above 900 °C.

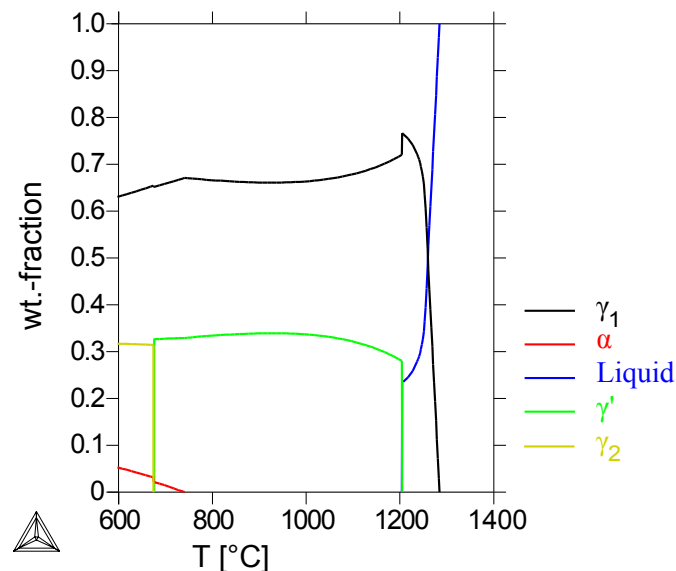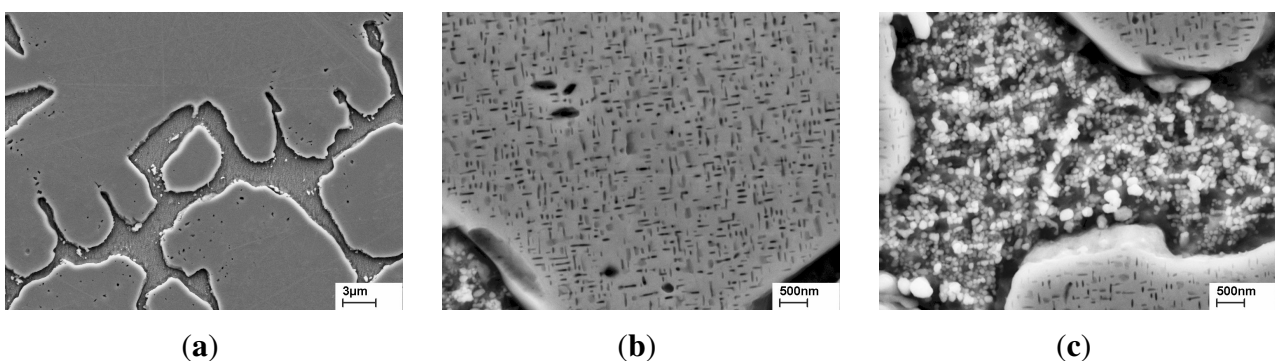**Figure 8.** Thermo-Calc calculations for the alloy Ni-30%Cu-22%Cr.

Figure 9. SEM-images (secondary electrons) of the alloy Ni-30%Cu-22%Cr after different heat treatments. Etched with molybdic acid. (**a**) Homogenization (1000 °C, 4 h); (**b**) 800 °C, 4 h, plate-shaped precipitates in the dendritic area; (**c**) 800 °C, 4 h, spherical precipitates in the interdendritic area.

(**a**)   (**b**)   (**c**)

After heat treatment at 800 °C (Figure 9(b)), plate-shaped precipitates in the γ_1-phase were observed, which are etched by molybdic acid. In the interdendritic area, spherical precipitates are formed, which are not etched by molybdic acid. Due to the small particle-size, no EDX analysis was possible, since the resolution of EDX is limited to the micrometer scale. The Thermo-Calc calculations showed a decrease of Cu- and an increase of Ni-content in the γ_1-phase with lower temperatures (Figure 10(b)). Therefore, a Cu-rich phase may form out of the γ_1-phase by heat treatment at 800 °C. Since the precipitates in Figure 9(b) are coherent and no phase transition is predicted, it can be assumed that this is the Cu-rich

γ'-phase, like in the interdendritic area at 1000 °C. For the interdendritic area, the precipitation of a Ni-rich γ_1-phase could be assumed analogical.

Finally, the hardness of the alloy was measured. After annealing at 1000 °C, the alloy has nearly the same hardness (154 HV 1) as after heat treatment at 800 °C (158 HV 1). Hence, the nanoscale precipitates in the heat treated sample do not harden the material, so they must be coherent with a crystallographic structure and lattice parameter very similar to the matrix material. However, this is in conflict with the shape of the precipitates in the γ_1-phase, as one would expect a spherical or cubic shape of the precipitates in the absence of a lattice parameter misfit [14]. Thus, further work has to take place to elucidate the precipitation reaction taking place at 800 °C.

Figure 10. Phase compositions of the alloy Ni-30 Cu-22%Cr: measured with EDX and calculated with Thermo-Calc. (**a**) Calculated phase-compositions *vs.* measured compositions at 1000 °C; (**b**) calculated phase-compositions at 800 °C and 1000 °C.

(**a**)

(**b**)
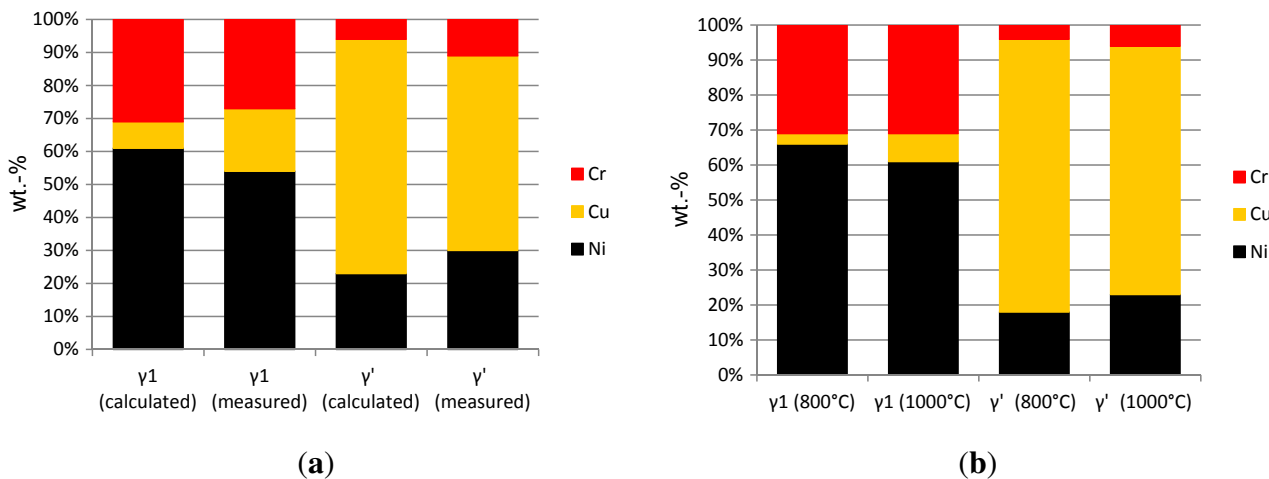
2.3. Ni-30%Cu-6%Al-5%Cr

In the previous section, an alloy without Al was investigated, where no α- and β-phase was observed. Although the Al might not be necessary in TBC-applications in rocket engines, this has not been demonstrated experimentally, so another possibility has to be considered, where an appropriate amount of Al is left to form an Al-oxide layer. In standard TBC-applications, the BC has to bring a large amount of Al and Cr to ensure a dense oxide layer over a long time, while the short heat exposure time in rocket engines does not make a large reservoir of Al and Cr necessary. To prove this experimentally, the Ni-30%Cu-alloy with Cr and Al content alike superalloys, in this case 6% Al and 5% Cr, was investigated.

The Thermo-Calc calculations shown in Figure 11 predict a two-phase γ_1/γ_2-microstructure with the formation of γ' below 1100 °C. Below 900 °C, a γ/γ'-microstructure is formed.
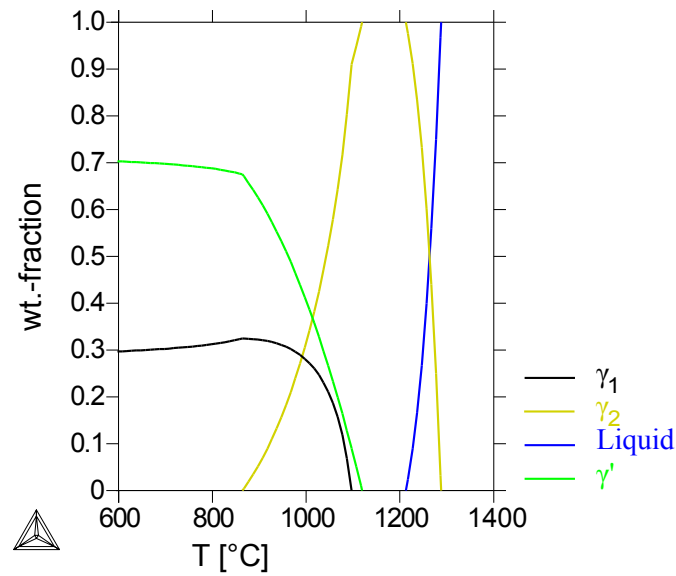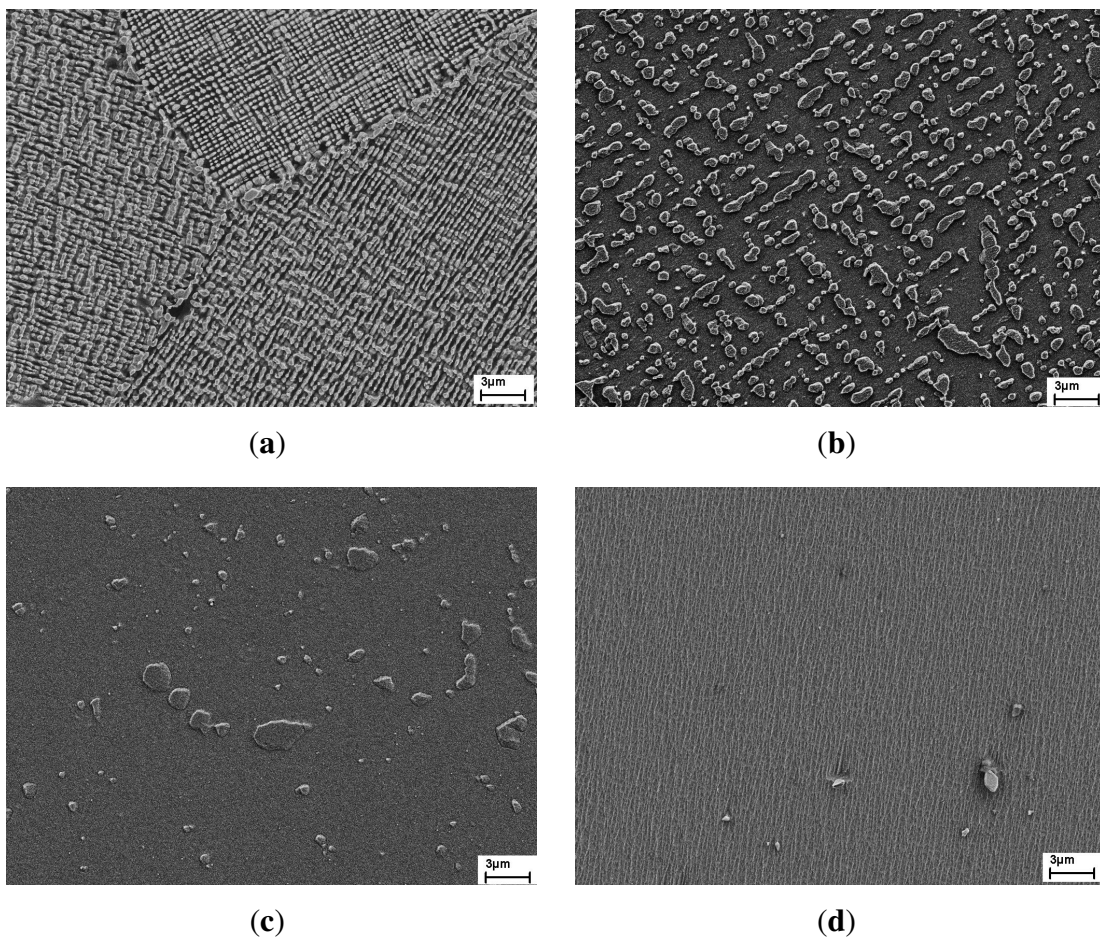
Figure 11. Thermo-Calc calculations for the alloy Ni-30%Cu-6%Al-5%Cr.

Figure 12. SEM-images (secondary electrons) of the alloy Ni-30%Cu-6%Al-5%Cr after different heat treatments. Etched with Adler-reagent. (**a**) 800 °C, 100 h; (**b**) 900 °C, 100 h; (**c**) 950 °C, 100 h; (**d**) 1000 °C, 100 h.

(**a**)

(**b**)

(**c**)

(**d**)

Figure 12 shows the microstructure after different heat treatments. At 1000 °C, the material is nearly homogeneous with only a few precipitates with a size of approximately 1 μm. At lower temperatures, more of the second phase precipitates up to a volume fraction of approximately 50% at 800 °C. At 900 °C and below, the particles align themselves in a continuous pattern over the entire grain, so the precipitates must be coherent to the matrix phase. Though the resolution of EDX is in the range of the particle size at 950 °C, the measurements showed a higher Al-content and lower Cu-content in the precipitates compared to the matrix. Considering the Thermo-Calc calculations and the fact that the second phase has a higher Al-content than the matrix and precipitates coherently, the microstructure below 1000 °C can be identified as γ/γ'.

Calorimetric measurements show a reaction with small latent heat between 700 °C and 1000 °C, related to the precipitation of the γ'-phase. The solidus temperature of the alloy is 1260 °C.

Furthermore, the coefficient of thermal expansion was measured. Figure 13 shows the CTE related to room temperature of the alloy Ni-30%Cu-6%Al-5%Cr compared to the CTE of NiCrAlY-alloys used in previous studies and copper as the substrate. The CTE of the NiCuCrAl-alloy is about $2 \times 10^{-6} \mathrm{K}^{-1}$ below the CTE of copper at room temperature and at 800 °C. In the range of 300 °C to 800 °C, the CTE is up to $5 \times 10^{-6} \mathrm{K}^{-1}$ below the CTE of the Cu-alloy. At higher temperatures, the CTE-difference is even lower than $2 \times 10^{-6} \mathrm{K}^{-1}$. However, the CTE-difference between CuNiCrAl and the copper substrate will be lower compared to the NiCrAlY-alloy used in previous studies. The lower value of the CTE below 800 °C is probably caused by the forming/dissolution of the γ'-phase.

Figure 13. Coefficient of thermal expansion related to room temperature of Ni-30%Cu-6%Al-5%Cr, Cu [24] and plasma-sprayed NiCrAlY [7].
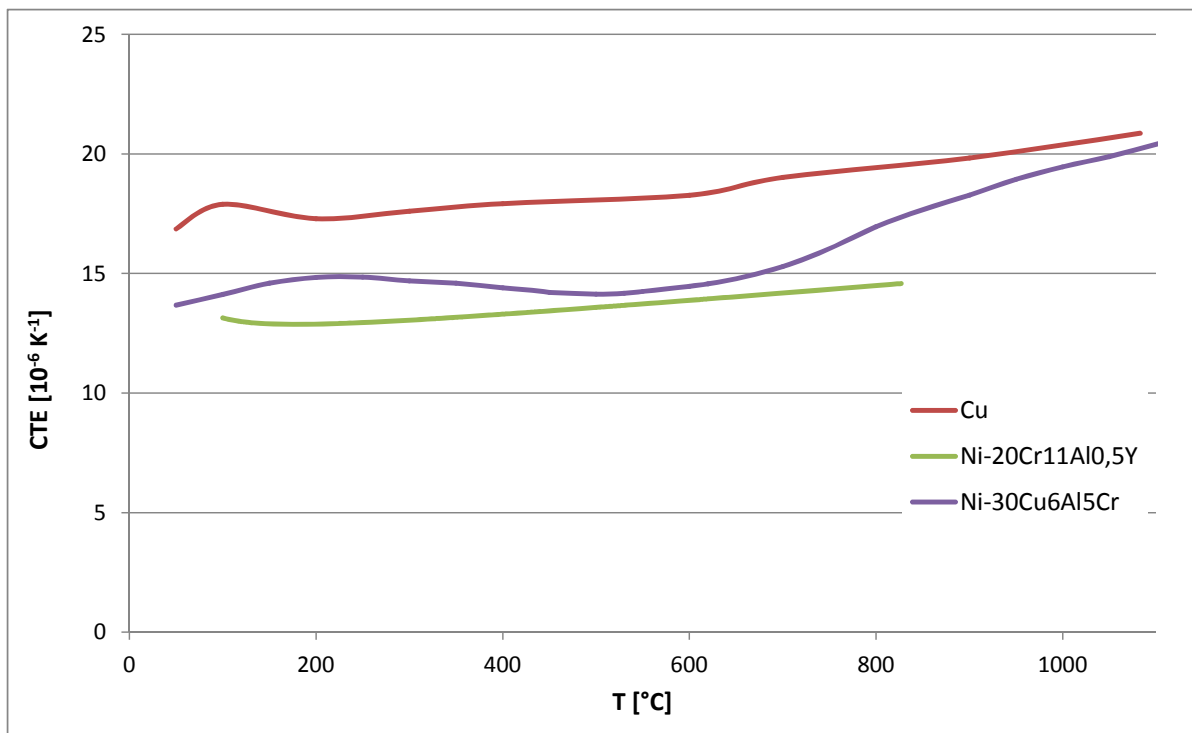
3. Materials and Methods

CALPHAD calculations were carried out with the software-package, Thermo-Calc [17], and the TTNI7-database. Although the database contains the involved elements and more than 30 possible phases, it is optimized to calculate Ni-based superalloys. Because a Cu-content of 30% is unusual for these alloys, the calculated phase compositions can only be considered as estimates and have to be verified experimentally.

For experimental investigation, the chosen alloys (see Table 1) were prepared using a Cu-30%Ni (wt%) pre-alloy and Cu, Ni, Cr, Al raw materials in a plasma-beam cold hearth melter and cast as rods with a diameter of 13 mm. The samples were subsequently homogenized at 1000 °C for 4 h. To evaluate the influence of Cu on the microstructure of NiCrAl-alloys, the samples were analyzed after homogenizing and after heat treatment at 800 °C for 4 h and 100 h, respectively. For the alloy Ni-30%Cu-6%Al-5%Cr, additional heat-treatments at 900 °C, 950 °C and 1000 °C were carried out for 100 h. All samples were quenched in water after every heat treatment.

Table 1. Compositions of the alloys investigated in this work (in wt%).

Nickel	Copper	Chromium	Aluminum
68	– –	22	10
38	30	22	10
48	30	22	– –
59	30	5	6

Optical microscopy, scanning electron microscopy (SEM) and energy-dispersive X-ray spectroscopy (EDX) were carried out to investigate the microstructure. Some samples were etched with molybdic acid reagent [18] consisting of 100 mL H_2O (dest.), 100 mL HNO_3 (65%), 100 mL HCl (37%) and 3 g MoO_3. The alloy Ni-30%Cu-6%Al-5%Cr was etched with the Adler-reagent (3 g copper-ammonium-chloride, 25 mL H_2O (dest.), 50 mL HCl and 15 g Iron(III)-chloride [19]).

Phase transitions and melting temperatures were identified by differential scanning calorimetry (DSC) using a Netzsch STA 449F3 calorimeter. The samples were homogenized and then heat-treated for 4 h at 800 °C and turned to rods with a 4-mm diameter and a height of 1 mm. They were heated up to 1370 °C with a heating-rate of 10 K·min^{-1} in an inert-gas atmosphere.

Dilatometric measurements were carried out to determine the coefficient of thermal expansion. The cylindrical sample with a diameter of 5 mm and a length of 43 mm was heated up from room temperature to 1120 °C with a heating rate of 1 K·min^{-1}.

The hardness was measured via Vickers indentation with a force of 9.8 N and an indentation time of 15 s.

4. Conclusions

In this study, the influence of copper on the microstructure of NiCrAl bond-coat alloys has been analyzed. The reference alloy Ni-22%Cr-10%Al was modified by adding copper. Since a large amount

of α-Cr and β-NiAl was found in the microstructure at an amount of 30% copper, two alloys were investigated, where neither α-Cr nor β-NiAl was expected: the aluminum-free alloy Ni-30%Cu-22%Cr and an alloy with a reduced Al and Cr content, Ni-30%Cu-6%Al-5%Cr. The main results can be summarized as follows:

- The addition of up to 30% copper to the reference NiCrAl alloy stabilizes the α-Cr phase.
- The Ni-30%Cu-22%Cr alloy has a two-phase microstructure with a phase transition between 800 °C and 1000 °C. This phase reaction has to be elucidated in further work.
- The Ni-30%Cu-6%Al-5%Cr alloy has a fcc-γ microstructure after homogenization. Below 1000 °C, a γ/γ'-microstructure was observed.
- The CTE of the NiCuCrAl alloy is only about $2 \times 10^{-6} \mathrm{K}^{-1}$ below the CTE of copper. The CTE-difference between copper substrate and the NiCuCrAl-bond coat will be lower compared to NiCrAlY bond-coats.
- Furthermore, Thermo-Calc has a sufficient reliability to allow the study of CuNiCrAl alloys.

Acknowledgments

Author Contributions

To.F., Ta.F., J.R. and M.B. conceived and designed the experiments, T.F. performed the experiments, To.F., Ta.F., J.R. and M.B. analysed the data; To.F. wrote the paper.

Conflicts of Interest

The authors declare no conflict of interest.

References

1. Schloesser, J.; Kowollik, D.; Bäker, M.; Rösler, J.; Horst, P. Thermal Barrier Coatings in Rocket Engines-A Multiscale Simulation and Development Approach. In *Sonderforschungsbereich/Transregio 40-Annual Report 2011*; SFB/TRR 40: Garching, Germany, 2011; pp. 207–219.
2. Riccius, J.; Haidn, O.; Zametaev, E. Influence of Time Dependent Effects on the Estimated Life Time of Liquid Rocket Combustion Chamber Walls. In *Proceedings of the 40th AIAA/ASME/SAE/ASEE Joint Propulsion Conference and Exhibit*; AIAA: Fort Lauderdale, FL, USA, 2004.
3. Ogbuji, L. A table-top technique for assessing the blanching resistance of Cu alloys. *Oxid. Met.* **2005**, *63*, 383–399.
4. Ogbuji, L.U. Oxidation behavior of Cu-Cr environmental barrier coatings on Cu-8Cr-4Nb. *Surf. Coat. Technol.* **2005**, *197*, 327–335.

5. Raj, S.V.; Ghosn, L.J.; Robinson, C.; Humphrey, D. High heat flux exposures of coated GRCop-84 substrates. *Mater. Sci. Eng. A* **2007**, *457*, 300–312.

6. Schloesser, J.; Bäker, M.; Rösler, J. Laser cycling and thermal cycling exposure of thermal barrier coatings on copper substrates. *Surface Coat. Technol.* **2011**, *206*, 1605–1608.

7. Taylor, T.; Walsh, P. Thermal Expansion of MCrAlY Alloys. *Surface Coat. Technol.* **2004**, *177–178*, 24–31.

8. Touloukian, Y.; Kirby, R.; Taylor, R.E.; Desai, P.D. *Thermophysical Properties of Matter Alloys 12 - Thermal Expansion - Metallic Elements and Alloys*; IFI/Plenum New York: Washington, DC, USA, 1975.

9. White, G.; Minges, M. Thermophysical Properties of Some Key Solids: An Update. *Int. J. Thermophys.* **1997**, *18*, 1269–1327.

10. Dies, K. *Kupfer und Kupferlegierungen in der Technik*; Springer-Verlag: Berlin/Heidelberg, Germany, 1967.

11. Sung, P.K.; Poirier, D.R. Estimation of densities and coefficients of thermal expansion of solid Ni-base superalloys. *Mater. Sci. Eng. A* **1998**, *245*, 135–141.

12. Schloesser, J.; Kowollik, D.; Bäker, M.; Rösler, J.; Horst, P. Sensitivity Analyses and Coating Development of Thermal Barrier Coatings in Rocket Engines. In *Sonderforschungsbereich/ Transregio 40 - Annual Report 2012*; SFB/TRR 40: Garching, Germany, 2012; pp. 209–218.

13. Massalski, T.B. *Binary Alloy Phase Diagrams*; American Society for Metals: Metals Park, OH, USA, 1986.

14. Bürgel, R.; Maier, H.J.; Niendorf, T. *Handbuch Hochtemperatur-Werkstofftechnik*; Vieweg Verlag: Wiesbaden, Germany, 2011.

15. Ma, K.; Tang, F.; Schoenung, J.M. Investigation into the effects of Fe additions on the equilibrium phase ccomposition, phase fractions and phase stabilities in the Ni-Cr-Al system. *Acta Mater.* **2010**, *58*, 1518–1529.

16. Durand-Charré, M. *The Microstructure of Superalloys*; Gordon and Breach Science Publishers: Amsterdam, The Netherlands, 1997.

17. Shi, P.; Sundman, B. *Thermo-Calc Database Guide*; Foundation of Computational Thermodynamics: Stockholm, Sweden, 2010.

18. Schumann, U.; DelGenovese, D.; Rösler, J. Auswahl der Ätzmedien für Ein- und Polykristalline Hochtemperaturwerkstoffe. *Praktische Metallographie Sonderband* **2004**, *36*, 269–274.

19. Schrader, A. *Ätzheft*; Gebr. Borntraeger: Berlin-Nikolassee, Germany, 1957.

20. Achar, D.; Munoz-Arroyo, R.; Singheiser, L.; Quadakkers, W.J. Modelling of phase distributions in MCrAlY coatings and their interactions with nickel based alloys. *J. Phys. IV France* **2004**, *120*, 231–238.

21. Köster, W.; Zwicker, U.; Moeller, K. Mikroskopische und röntgenographische Untersuchung zur Kenntnis des Systems Kupfer-Nickel-Aluminum. *Zeitschrift für Metallkunde* **1948**, *39*, 225–231.

22. Raj, S.; Palczer, A. Thermal Expansion of Vacuum Plasma Sprayed Coatings. *Mater. Sci. Eng. A* **2010**, *527*, 2129–2135.

23. Gupta, K.P. *Phase Diagrams of Ternary Nickel Alloys*; Indian Institute of Metals: Calcutta, India, 1990.

24. Kupferinstitut, D., Ed. *Kupferdatenblatt CuCr1Zr*; Deutsches Kupferinstitut, Düsseldorf, Germany, 2005.